RSC Advances

ROYAL SOCIETY OF CHEMISTRY

www.rsc.org/advances

Cite this: DOI: 10.1039/c0xx00000x

www.rsc.org/xxxxxx

ARTICLE TYPE

A novel TiO_2-assisted magnetic nanoparticle separator for treatment and inactivation of bacterial contaminants in aquatic systems

Werner E. G. Müller,*[a] Thorben Link,[a] Qiang Li,[b] Heinz C. Schröder,[a] Renato Batel,[c] Maria Blažina,[c] Vladislav A. Grebenjuk[a] and Xiaohong Wang*[a]

Received (in XXX, XXX) Xth XXXXXXXXX 20XX, Accepted Xth XXXXXXXXX 20XX
DOI: 10.1039/b000000x

Ferromagnetic nanoparticles (Fe-nanoparticles) have been functionalized with recombinant poly-Glu [glutamic acid]-tagged silicatein, a biomineral-synthesizing enzyme from siliceous sponges that forms the inorganic silica skeleton of those animals. The biocatalytic activity of silicatein was used to form a titania (TiO_2) shell around the iron nanoparticle core, using the water-soluble non-natural substrate titanium bis(ammonium lactato)-dihydroxide (TiBALDH). Thereby the diameter of the nanoparticles increases from 7 nm to ≈22 nm. This procedure also allows the layer-by-layer fabrication of titania/silica-Fe-nanoparticles. SEM/EDX analysis confirmed the presence of the Ti and Si signals in the resulting titania-Fe-nanoparticles and titania/silica-iron nanoparticles, besides the dominant Fe signal. Utilizing the photocatalytic and ferromagnetic properties of the titania-Fe-nanoparticles a method has been developed for cleaning aquatic systems from bacterial contaminants. For that purpose, a novel magnetic nanoparticle separator has been constructed, with a motor-driven coil stirrer submersed into the reaction tube that contains, besides of the bacteria, the titania-Fe-nanoparticles. This device enables the irradiation of contaminated water samples with UV-A light in order to initiate the photocatalytic reaction mediated by the titania-Fe-nanoparticles, resulting in the killing of the bacteria. At the end of the reaction, the iron nanoparticles can be recovered from the solution by applying an electromagnetic force, leaving behind the bacterial remains. This photocatalytic method and the magnetic nanoparticle separator allow a fast and efficient elimination of bacteria from aqueous solution and can be applied for remediation of aquatic environments.

1 Introduction

The usefulness of iron nanoparticles as a vehicle for targeted decontamination processes is well documented.[1] Those nanoparticles can bind either a broader range spectrum of dissolved inorganic ions and molecules by physico-chemical adsorption, absorption or chelation, e.g. as shown initially for arsenic.[1] Basically, those adsorption processes are comparable with the use of functional groups linked to matrices or ion exchangers.[2-4] The utilization of iron nanoparticles for the remediation of the environment is attractive because of the straightforward separation feasibility, based on magnetic attraction and – by that – collection of the loaded nanoparticles for waste disposal and management.[5] In the following, ferromagnetic nanoparticles have been successfully introduced as recyclable adsorbent in aqueous environmentally contaminated/polluted milieu.[6,7] The nanoparticles are superior to functionally larger active surfaces or filters due to their drastically larger active surface areas per weight of matrix, the very high surface to volume ratio.[8]

Usually the dispersion of the particles to nanosize dimensions, prior to magnetic separation is typically not verified (reviewed in: ref. 8); in reality the nanoparticles are arranged to aggregates, causing a turbid appearance of the dispersion. This problem can be overcome by a functionalization of the surfaces and – by that – an overcome of the electrostatic forces between the particles by turning their surfaces to hydrophilic residues, causing a repulsion of the particles.[9]

Besides of dissolved inorganic and organic ions and molecules the aqueous milieu is heavily loaded with microorganisms, bacteria [usually > 10^6 mL^{-1}][10] and viruses [likewise ≈$10•10^6$ viruses per milliliter of surface seawater][11]. It should be stressed on this point that in some instances bacterial bioremediation, e.g. by using mercury-resistant bacteria, is advantageous.[12] Very efficient in the elimination of bacteria from the marine environment are some filter feeder animals, e.g. sponges, that can eliminate almost all bacteria from the water circulating through their body.[13] However, many bacterial toxins are produced that are harmful for the biotic ecosystem in general[14] and to humans in particular[15]. Besides of mechanical cleaning, chlorination and ozonation have been proposed to help to reduce the load of bacteria and organic matter in the marine wastewater.[16] Accompanying to these procedures, dose-controlled ultraviolet irradiations have been proposed.[17]

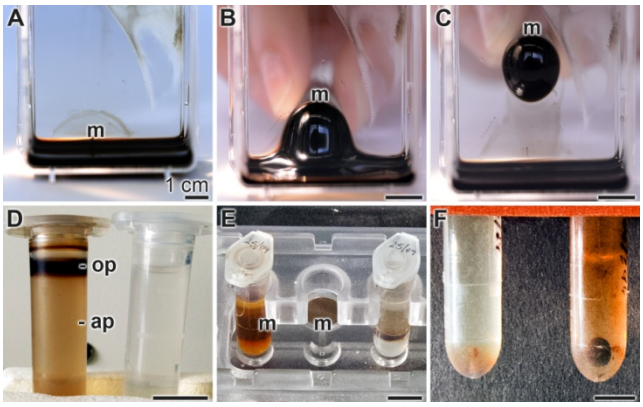

Fig. 1 Preparation of silicatein-Fe-nanoparticles. (**A** to **C**) In the first step iron nanoparticles are prepared that are covered with an oleic acid layer. They can readily be translocated in organic (ethanolic) suspension using a round disc circular magnet (m). (**D**) (Left tube) The surface of the organic-coated nanoparticles has been functionalized with -COOH groups, by suspending them in hexane and subsequent exposure to acetic acid. After reaction the bulk of nanoparticles is suspended in the aqueous phase (ap), while the non-reacted oleic acid-covered particles are attached to the plastic surface of the Eppendorf tube in the upper, organic phase (op). (Right) The reaction process has been performed in the absence of iron(III) chloride; the sample remains non-colored and pellucid. (**E**) Separation of the iron nanoparticles by vertically fixed magnet (m). Left: Suspension with silicatein-Fe-nanoparticles, formed during the reaction; middle: Orientation of the magnet; right: Assay without added iron(III) chloride. (**F**) Assay with (left) or without iron nanoparticles (right). The nanoparticles are vertically attached through the forces of the vertically fixed magnet. All size bars measure 1 cm.

Now we apply ferromagnetic nanoparticles that are covered by silica or titania as functional coatings with a purpose to be introduced in the remediation of aqueous environmental systems. Both oxides have been enzymatically deposited onto the ferromagnetic nanoparticles, using silicatein from sponges.[18; reviewed in: ref. 19,20] These animals (phylum: Porifera) use this enzyme to fabricate their siliceous skeletons.[21] Focusing on silica it is known that this polymer, especially if formed in a sol-gel process, adsorbs toxic compounds.[22] In a future series of experiments this application will be studied in a greater detail. In the present study we propose that titania (TiO_2), prepared from the titanium bis(ammonium lactato)-dihydroxide precursor *via* silicatein, can be used to efficiently eliminate bacteria from the aquatic environment. Titania is well established and commercially extensively used component in semiconductor technology.[23] In addition, this inorganic material has been proven to be photocatalytically active and can kill bacteria.[24-26] This toxic effect of titania is attributed to the production of reactive oxygen species (ROS) that inactivate and kill the bacteria.[27] During the photocatalytic mechanism of the water-splitting reaction hydrogen and oxygen are formed; in parallel hydroxyl radicals and superoxide ions are produced when illuminated under UV light. In turn, photocatalysts coupled to UV lights have the potency to oxidize organic pollutants into nontoxic materials (e.g. CO_2 and water) and can disinfect bacteria in water. This technology can also be effectively applied to remove hazardous organic compounds and kill bacteria and viruses in the secondary wastewater.

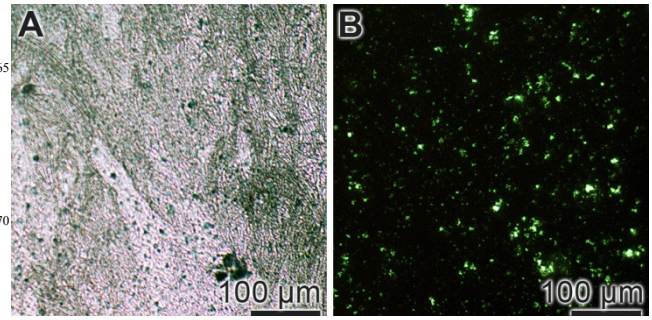

Fig. 2 Reaction of the silicatein-Fe-nanoparticles, layered on a glass slide (**A**) with anti-silicatein antibodies (**B**). The immunocomplexes formed (A) are highlighted with the labeled secondary antibodies (B).

In the present study we apply a technology to fabricate titania-iron nanoparticles and show that those particles efficiently kill bacteria. In turn, we propose that this technology may represent an alternative to the use of chlorine-based oxidants, ozonation and short wavelength UV-C irradiation as a method to remediate aqueous systems from microorganisms. As light source we used illuminating UV-A light source (wavelength λ_{max}: 365 nm), known to kill bacteria, e.g. *Escherichia coli*, *Staphylococcus aureus*, *Pseudomonas putida* and *Listeria innocua*, if having contact to TiO_2-coated surfaces.[28] In the home-made magnetic nanoparticle separator we could demonstrate an effective procedure to kill bacteria by titania-coated nanoparticles, through a photocatalytic reaction. Those nanoparticles can be re-used by a straightforward magnetic collection procedure.

2 Results

2.1 Ferromagnetic nanoparticles covered with Glu-tagged silicatein

In the first step iron nanoparticles were prepared as iron oleate complex nanoparticles. The iron nanoparticles formed have an average size of approximately 7 nm. They display strong magnetic properties (Fig. 1A to C). The hydrophobic surface residues had to be replaced by -COOH groups in order to allow a coating of the ferromagnetic particles with silicatein. The separation of the two phases, organic layer from the aqueous layer, can be readily performed (Fig. 1D). The non-reacted particles remain attached at the surface of the tubes within the organic phase. The particles are stained brownish/darkish, while the solution of the control assay lacking the iron precursor remains translucent.

After transfer of the oleate ferromagnetic particles to acetic acid they can be covered by Glu-tagged silicatein. The silicatein-Fe-nanoparticles can be readily suspended and concentrated in a matching manner with the spatial dimension of the magnet (Fig. 1E and F). In Fig 1E and F reaction samples are shown during which no iron chloride had been added. During functionalization the size of the particles increases from ≈ 7 nm to 10-30 (in maximum) nm.

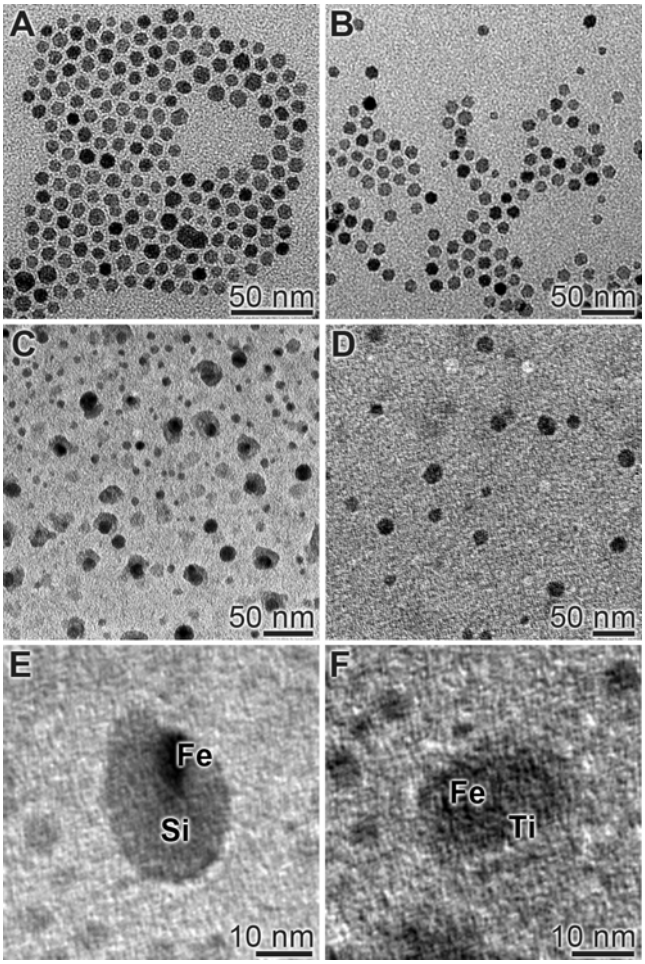

Fig. 3 Nanoparticles formed from iron(III)acetyl acetonate and oleic acid; TEM analysis. (**A**) Plain iron-oleate nanoparticles show a highly clustered and organized arrangement. (**B**) Iron nanoparticles whose surfaces are transferred from a hydrophobic to a hydrophilic property are arranged more irregular on the grid. Those hydrophilic nanoparticles have been covered with silicatein. (**C**) The silicatein-Fe-nanoparticles have been incubated with prehydrolyzed TEOS, allowing the formation of a silica mantel. (**D**) If the silicatein-Fe-nanoparticles are reacted with TiBALDH, the second substrate for this enzyme, an electron-dense coat around the iron nanoparticles is formed. Higher magnification both of a silica-coated iron nanoparticle (**E**) and a titania-coated iron nanoparticle (**F**). The formed enzymatically silica (Si) cover and titania (Ti) cover around the iron (Fe) nanoparticle are marked.

The nanoparticles, functionalized with Glu-tagged silicatein, can be spread onto a glass slide for reaction with antibodies against silicatein (Fig. 2). The silicatein-Fe-nanoparticles (Fig. 2A) highlight in green with the stained anti-silicatein antibodies (Fig. 2B).

2.2 Morphology of the particles

The plain iron-oleate nanoparticles show, due to their hydrophobic surface behavior, a highly clustered and organized arrangement, if they are inspected by TEM (Fig. 3A). There sizes are 6-8 nm. If they are transferred to hydrophilic particles by functionalization with -COOH groups the size of the particles does not change. If they become coated with silicatein-Fe-nanoparticles, the distribution of the particles becomes more irregular on the grid (Fig. 3B); their sizes vary between 10-14 nm. If the silicatein-Fe-nanoparticles become exposed with the substrate of the enzyme, with prehydrolyzed TEOS, the silica formed around the iron nanoparticles let the particles grow to 22 nm (20-25 nm) (Fig. 3C). If the enzyme, linked to the iron nanoparticles, reacted with TiBALDH a more electron-dense mantel around the iron nanoparticles is formed (Fig. 3D) with a slightly larger size of 22-26 nm. At a higher magnification it is apparent that the silica mantel around the iron particles is more translucent (Fig. 3E), compared to the almost opaque titania cover (Fig. 3F). The titania/silica-iron nanoparticles formed by layer-to-layer silicatein-directed syntheses of the silica and the titania coat have the same dimension of 25-30 nm (not shown).

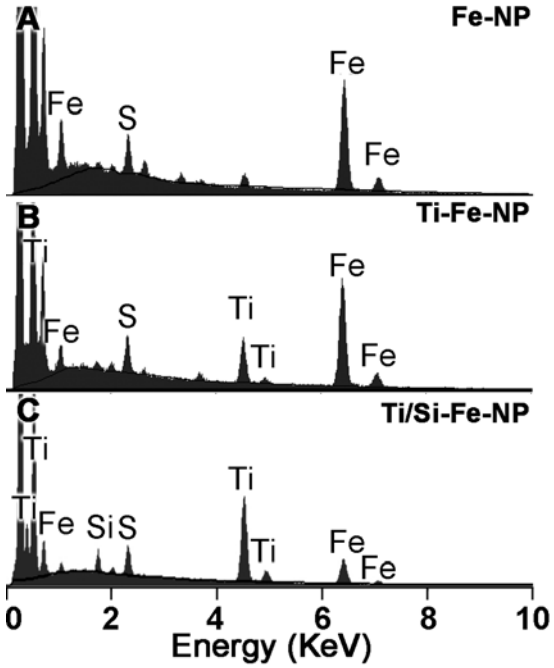

Fig. 4 EDX-based elemental analyses of clusters of silicatein-iron nanoparticles. Clusters of 5x5 µm areas of ferromagnetic particles (Fe-NP) (**A**), titania-Fe-nanoparticles (Ti-Fe-NP) (**B**), as well as of titania/silica-iron nanoparticles (Ti/Si-Fe-NP) (**C**) were analyzed. The element peaks for iron (Fe), sulfur (S) [originating from silicatein], titanium (Ti), as well silicon (Si) are shown.

2.3 EDX analysis of the ferromagnetic nanoparticles

The samples with the ferromagnetic particles, silicatein-Fe-nanoparticles, titania-Fe-nanoparticles, as well as the titania/silica-iron nanoparticles were analyzed by SEM/EDX. Clusters of particles, spanning an area of 5x5 µm were analyzed. In Fig. 4 the spectra for the ferromagnetic particles (Fig. 4A), for the titania-Fe-nanoparticles (Fig. 4B) as well as the titania/silica-iron nanoparticles (Fig. 4C) are shown. It is evident that the

ferromagnetic particles contain Fe as a dominant signal, while the titania-Fe-nanoparticles are characterized both by the Fe and the Ti signals. The titania/silica [layer-by-layer]-iron nanoparticles comprise both silicon, Ti and Fe signals.

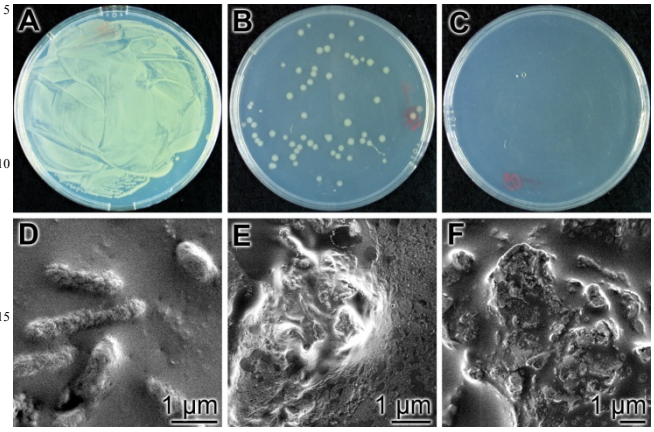

Fig. 5 Effect of UV light exposure on growth of *E. coli* on LB-Medium/LB-Agar medium, supplemented with 50 µg/mL of titania-Fe-nanoparticles. (**A**) Growth of the bacteria in the dark. A homogeneous layer of bacterial cultures is seen after 12 h. (**B** and **C**) The bacteria have been exposed to UV-A light for 2 h (B) or 4 h (C); an almost complete elimination of bacterial colonies is seen. (**D** to **F**) SEM analysis of *E. coli* grown in the absence of light for 12 h (D), or exposed to UV-A light for 2 h (E) and 4 h (F).

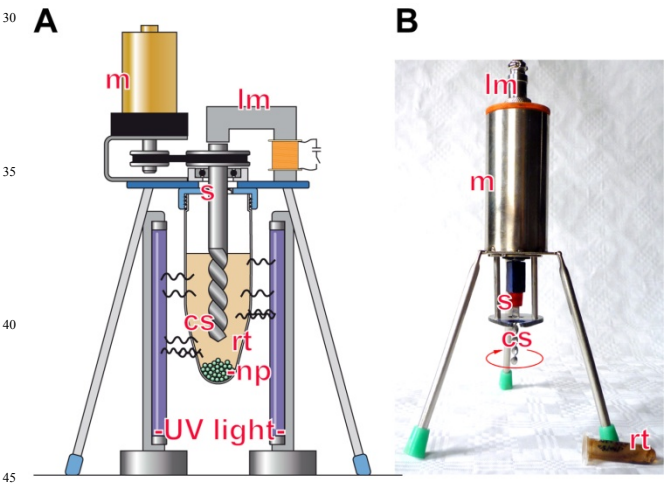

Fig. 6 Magnetic nanoparticle separator (**A** scheme; **B** device), suitable for killing of bacteria by the photocatalytic reaction proceeding on titania coated around iron nanoparticles. The reaction tube (rt), containing *E. coli* bacteria in medium, is supplemented with titania magnetic iron nanoparticles (np). The culture is stirred via a motor by a coil stirrer (cs). This stirrer is connected through a socket (s) with a motor (m). In order to collect the nanoparticles the system is connected with a lifting magnet (lm). In order to kill the bacteria the cell suspension is illuminated under UV-A light exposure (λ_{max}, 365 nm).

2.4 Reaction of *E. coli* to UV light

The bacteria were grown on LB-Medium/LB-Agar that was supplemented with 50 µg/mL of titania-Fe-nanoparticles, remained either in the dark, or were exposed to the UV-A light (λ_{max}: 365 nm) at a distance of 5 cm. If those cultures were incubated in the dark for 12 h the bacterial colonies grew to an almost homogeneous dense layer (Fig. 5A). However, if those cultures were exposed to UV-A light for 2 h (Fig. 5B) or 4 h (Fig. 5C), an almost complete growth inhibition is observed. If those cultures are inspected by SEM the morphology of the bacteria changed and turned from rod-shaped (Fig. 5D; in the absence of light) to partially (Fig. 5E) or completely fragmented bacterial membrane clusters (Fig. 5F).

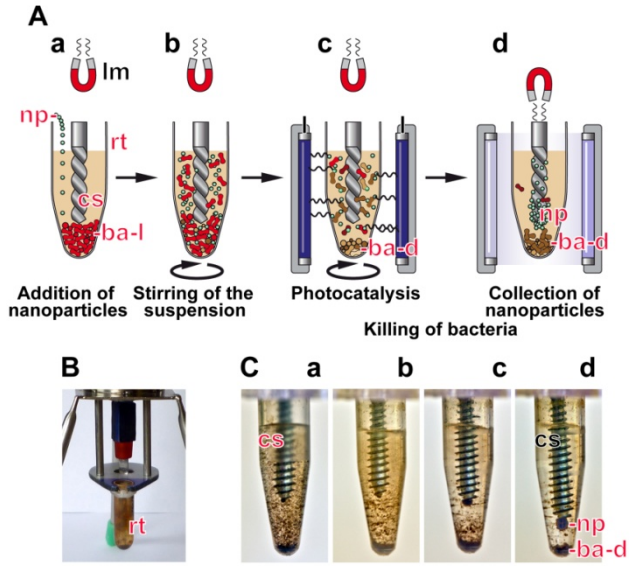

Fig. 7 Function of the magnetic nanoparticle separator. (**A**) Schematic outline of the killing process of bacteria due to the photocatalytic reaction on titania-Fe-nanoparticles. After addition of nanoparticles (np) and the living bacteria (ba-l) to the reaction tube (rt), the rotation of the coil stirrer is started. The resulting suspension is exposed to UV-A light (l) resulting in initiation of the photocatalytic reaction of the titania on the iron nanoparticles. Finally, the rotation of the coil stirrer is terminated and electromagnetic force is applied to remove the nanoparticles (np), leaving behind the dead bacteria (ba-d). (**B**) Close up of the reaction tube (rt) in the nanoparticle separator. (**C**) Course of the attraction of the titania-Fe-nanoparticles to the coil stirrer (cs). At the bottom of the reaction tube the dead bacteria (ba-d) are accumulating.

2.5 Photocatalytic killing of bacteria using a magnetic nanoparticle separator

We constructed a magnetic nanoparticle separator with the purpose of a photocatalytic killing and elimination of *E. coli*. As outlined under “Material and Methods” the Eppendorf reaction tube was placed into a small docking platform (Fig. 6). A coil stirrer was submersed into the reaction tube and turned around *via* a motor. The reaction tube contained, besides of the bacteria,

titania-Fe-nanoparticles. If wanted electromagnetic force was applied that pulled out the iron nanoparticles from the solution.

A schematic outline of the process is shown in Fig. 7A. The bacterial culture, suspended in LB-Medium, is supplemented with titania-Fe-nanoparticles (Fig. 7A-a). Then the suspension is mixed with a coil stirrer, connected with a motor (Fig. 7A-b). Then the system is exposed to UV-A light, resulting in an elimination of the bacteria, in response of a photocatalytic reaction, driven by titania that is surrounding the iron nanoparticles. During this process the bacteria are killed. After termination of the rotating of the coil stirrer and activation of the lifting magnet the nanoparticles are attracted and can be removed from the system. In Fig. 7B a close-up of the reaction tube with the coil stirrer that is hooked to the motor is shown. Finally, the process of attraction of the titania-Fe-nanoparticles to the coil stirrer after applying an electromagnetic force to the titania-Fe-nanoparticles is shown (Fig. 7C-a to 7C-d).

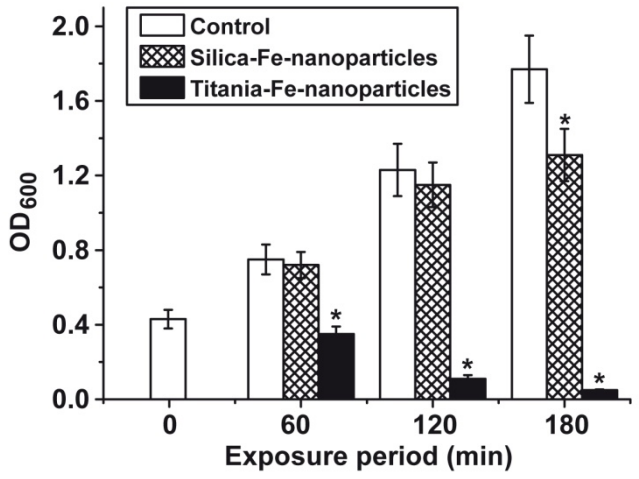

Fig. 8 Growth curves of *E. coli* cells measured after exposure to UV light to the magnetic nanoparticle separator. Cultures of *E. coli* in LB-Medium were supplemented with 50 µg/mL of titania-Fe-nanoparticles and then incubated in the absence of UV light (controls; open bars). In parallel, the bacterial suspension was supplemented with either silica- (silica-Fe-nanoparticles; hatched bars), or titania-coated iron nanoparticles (titania-Fe-nanoparticles; closed bars) and then exposed to UV light. After a total incubation period of 60 min, 120 min, or 180 min samples were taken and the optical density (OD_{600}) was determined. Values represent the means (±SD) from 10 separate experiments each (*$P < 0.01$).

2.6 Effect of photocatalysis on TiO_2 surfaces on iron nanoparticles

E. coli cells were suspended in 2 mL LB-Medium at an initial density of 0.2 (OD_{600}). The cell suspension was supplemented with 50 µg/mL of titania-Fe-nanoparticles and incubated in the absence of UV light for 180 min. After a pre-incubation period of 1 h, samples were taken and the optical density of the suspension was determined (Fig. 8). It is seen that the cell density of the culture, reflected by the optical density of the solution, is increasing from 0.43±0.05 (time 0) via 0.75±0.08 (after 60 min) to 1.23±0.14 (120 min). A similar growth kinetics is seen for the bacteria, growing in cultures with silica-Fe-nanoparticles, and exposed to light; the optical density increased from 0.4 (start) to 0.72±0.07 (60 min) and 1.15±0.12 (120 min) to finally 1.31±0.14 (180 min). Only after the longer incubation period of 180 min a slight, but significant reduction of bacterial growth, in comparison to the controls is measured.

In the assay with *E. coli* that was cultivated together with titania-Fe-nanoparticles in the nanoparticle separator and exposed to UV light, the bacteria showed a reduced growth and even cell death. After an exposure period of only 60 min the optical density is reduced from 0.4 (time 0) to 0.35±0.04. After an extended incubation period the die-off of the bacteria is even more pronounced to 0.11±0.02 (120 min) and 0.05±0.01 (180 min); Fig. 8. In controls it was established that bacteria growing with titania-Fe-nanoparticles, however in the absence of UV light, showed the same growth kinetics (not shown here).

3 Discussion

Nanoparticles have, in contrast to micro- or larger particles, or even to plates the inherent property to expose a comparatively ultralarge functionally-active surface. The 15 nm sized titania-Fe-nanoparticles display a surface of $7x10^{-10}$ mm^2, equivalent to $1.5x10^9$ particles per 1 mm^2, if compared with a plain planar and functionally reacting surface. In our assay system we added 50 µg of titania-Fe-nanoparticles, equivalent to $1x10^{13}$ [$9.43x10^{12}$] particles (suppose a density of 3 g/cm^3 for iron oxide) per mL assay. Taking a diameter of 30 nm, still $1.18x10^8$ particles are present in the 50 µg nanoparticle preparation. This impressive advantage of the nanoparticles with respect to their functional surface over planar plates or larger particles qualify the nanoparticles for an application in process technology with a maximum possible economically and spatial cost-effective utilization.

In the present study we succeeded to fabricate iron nanoparticles whose hydrophobic surface had been changed to a hydrophilic one allowing a strong ionic interaction[29] to the poly-Glu [glutamic acid]-tagged silicatein. In turn, the enzymatic function of the enzyme silicatein could be utilized to form around the iron nanoparticles either a silica mantel, by using prehydrolyzed TEOS as a substrate, or a titania mantel, if TiBALDH is used as a substrate. Through this coating process the size of the nanoparticles increased from ≈7 nm to 20 to 30 nm. By this process it could even be succeeded to fabricate layer-by-layer titania/silica-Fe-nanoparticles. Those particles – as expected[30,31] – comprise ferromagnetic properties allowing a straightforward attraction of the particles from the solution.

For the application-oriented studies summarized here the titania-Fe-nanoparticles have been applied to clean the aqueous environment in which the nanoparticles have been added. In the present study we took advantage of the photocatalytic property of titania and its effect to kill bacteria.[28,32] As a result of the discovery that titanium dioxide (TiO_2) can clean water by photoinduction.[33] This catalyst, titania/titanium dioxide/titanium(IV) oxide, gained increasing interest not only as a semiconductor material but also as an environmentally friendly material applicable for purification of water and air.[reviewed in: ref. 34; 35-37] If illuminated with UV light with wavelengths of < 385 nm,

titania generate strong oxidizing power due to photocatalysation. Via holes (H^+) and hydroxyl radicals ($OH^•$), formed in the valence band, and electrons and superoxide ions (O_2^-), produced in the conduction band, titania decomposes and mineralizes organic compounds through a series of oxidation reactions. In line with earlier studies, demonstrating that bacteria are killed on TiO_2/SiO_2 platforms (e.g. ref. 38), it is shown here that titania-Fe-nanoparticles added to the culture broth/agar rapidly kills the bacteria (*E. coli*) after exposure to UV light.

This property of photocatalytic killing and disinfection of *E. coli* suspensions by titania is retained if titania is surrounded around the Fe-nanoparticles. If those particles are added to *E. coli*, growing in suspension in a reaction tube inserted into a magnetic nanoparticle separator, and exposed to UV light, the cells are prevented from growth, even more they are lethally affected and die away. During the incubation under light the nanoparticles can randomly directed *via* Brownian forces but especially as a result of the directing rotating coil stirrer the nanoparticles can reach the space of the incubation tube. The attractive aspect of this magnetic nanoparticle separator is that after a relatively short operating time the titania-Fe-nanoparticles can be collected from the bacterial cultures, leaving behind the bacterial remains. Under the incubation conditions and cell concentrations used, no filtration of the assays had been necessary reach the goal. In addition, the system allows the application of diversified functionalized nanoparticles, especially iron nanoparticles, e.g. by the use of the iron nanoparticles, coated with the silica adsorbent. As shown in the present study also silica-Fe-nanoparticles can be prepared by the catalytic function of silicatein, starting from the prehydrolyzed TEOS. Those silica surfaces around magnetic nanoparticles have been shown to bind, after functionalization with cetylpyridinium bromide heavy metals, e.g. Cd(II), Co(II), Cu(II),Mn(II), Ni(II), or Pb(II) from the water samples.[39,40]

4 Material and Methods

4.1 Materials

The sources for the enzymes and reagents, used for the molecular biological experiments, were listed previously.[41]

4.2 Recombinant silicatein (Glu-tagged silicatein)

The recombinant protein of silicatein (SILICa_SUBDO) was prepared from the short form of the mature silicatein-α of *Suberites domuncula*.[42,43] In short, the silicatein-α cDNA (accession number CAC03737.1) with a forward primer 5'-CATGCCATGGTGGAAGAGGAAGAGGAAGAGGAAGAGC CTGAAGCTGTAGACTGG-3' and a reverse primer 5'-CCCAAGCTTATTAGGGTGGGATAAGATGCATCGGT-3' was used to generate the recombinant 8x Glu-tagged silicatein. The cDNA was ligated into the expression vector pBAD/gIII A (Invitrogen, Karlsruhe; Germany) and used for transformation of TOP10 *Escherichia coli* cells (Invitrogen, Karlsruhe; Germany). Expression was induced with arabinose (0.2%) for 24 h, followed by the extraction of the protein. The recombinant Glu-tagged silicatein was purified by affinity chromatography, unfolded in 6 M urea/5 mM imidazole and finally refolded in 50 mM Tris/HCl buffer (0.5 M L-arginine, glutathione [9 mM glutathione / 1 mM oxidized glutathione] redox couple, 0.3 M NaCl, 1 mM KCl).[44] The final protein concentration was 110-130 µg mL^{-1}.

4.3 Determination of the enzymatic activity of silicatein

The standard enzyme assay was composed as given before.[42,44] In a typical assay, samples of 1 mL were prepared in 50 mM Tris/HCl buffer (pH 7.4; 150 mM NaCl) containing 6 µg of purified recombinant silicatein. The enzyme preparation was supplemented with 200 µM substrate, prehydrolyzed TEOS (tetraethyl orthosilicate, #759414; Sigma, Taufkirchen; Germany). Acid hydrolysis was performed as previously described,[45] with a 1:5 molar ratio of TEOS/H_2O in 10 mM HCl for 10 min. The reactions were run at 22°C for 1 h under shaking. To determine the amount of biosilica formed, the samples were centrifuged (10,000 ***g***, 30 min, 4°C) and, after washing with ethanol, the sedimented biosilica was treated with 2 M NaOH for 30 min (30°C) to hydrolyze biosilica formed. Then the concentration of the liberated, soluble silicic acid was determined applying the molybdenum blue colorimetric method[46] and using the Silicon Test colorimetric assay kit (#1.14794, Merck Darmstadt; Germany). A calibration curve with a silicon standard (#1.09947 Merck) was established to calculate the absolute amounts of silicic acid from the obtained absorbance values at 795 nm. The specific activity was ≈ 12 µg biosilica formed $µg^{-1}$ enzyme protein during an incubation period of 1 h.

4.4 Synthesis of ferromagnetic nanoparticles

The preparation of magnetic iron oxide nanoparticles was performed as described.[9,30,31] In brief, an iron oleate complex was prepared from 2 mmol iron(III)acetyl acetonate [$Fe(acac)_3$] that was mixed with 20 mL of benzyl ether, followed by addition of 10 mmol 1,2-hexadecanediol, 6 mmol oleic acid and finally 6 mmol oleylamine under argon atmosphere and heated to 200°C at a heating rate of 5°C per min to reflux for 30 min. The dark-brown solution was cooled to room temperature and the particles were precipitated with ethanol. The magnetite nanoparticles produced had a size of ≈7 nm. They were found to be monodisperse, as analyzed by scanning electron microscopy.

The iron nanoparticles could be conveniently attracted and translocated in the organic or aqueous environment with a round disc circular magnet 18 x 10 mm (rare earth neodymium).

4.5 Functionalization of ferromagnetic nanoparticles with silicatein

In order to make the hydrophobic nanoparticles water-dispersible and to replace the oleic acid layer surrounding the particle surface[47] the particles (500 mg) were suspended in hexane, containing 0.1% acetic acid, under rotation (72 hr) to facilitate the ligand exchange reaction. Then the suspension was briefly sonicated and the precipitate formed was collected, washed twice with ethanol, and then resuspended in 5 µg mL^{-1} of Glu-tagged silicatein, dissolved in 50 mM Tris/HCl buffer. After incubation for 24 h Glu-tagged silicatein iron nanoparticles [silicatein-Fe-nanoparticles] were recovered and purified using a magnet-based separator (MagnaRack CS15000; Invitrogen).

4.6 Layering of the ferromagnetic particles with silica and titanium

The ferromagnetic particles, functionalized with silicatein, the silicatein-Fe-nanoparticles, were incubated with prehydrolyzed TEOS, using the assay conditions described above. A suspension of iron nanoparticles in the 50 mM Tris/HCl buffer was incubated with 200 µM prehydrolyzed TEOS for 12 h. Then the particles formed were sedimented with a magnet at the bottom of tube then suspended again in distilled water; they were termed "silica-Fe-nanoparticles".

"Titania-Fe-nanoparticles" were prepared in the same way. The iron nanoparticles were incubated with 250 µM titanium bis(ammonium lactato)-dihydroxide (TiBALDH; Sigma-Aldrich #388165) under the same conditions,[48] like described for the silica-Fe-nanoparticles.

In one series of experiments layer-by-layer ferromagnetic particles have been prepared by a sequential combination of the coating process. At first silica-Fe-nanoparticles were prepared. After washing them they were transferred to the 250 µM TiBALDH containing assay system. The incubation period was again terminated after 12 h. The particles are termed "titania/silica-iron nanoparticles".

4.7 Immunostaining of the silicatein-Fe-nanoparticles

Antibodies against the *S. domuncula* recombinant silicatein-α were prepared in rabbits.[49] The silicatein-Fe-nanoparticles were applied onto a glass slide and reacted with polyclonal antibodies (1:2000 dilution). After washing and blocking with goat serum (Invitrogen) the samples were incubated with the anti-silicatein antibodies. The immunocomplexes we visualized by reaction with fluorescently labeled (Cy3 [green]; Dianova, Hamburg; Germany) secondary antibodies (dilution 1:3000). Antibodies, adsorbed with recombinant silicatein, did not show any reaction to the silicatein-Fe-nanoparticles (not shown).

4.8 Electron microscopy/energy-dispersive X-ray spectroscopy

Samples of ferromagnetic particles, silicatein-Fe-nanoparticles, silica-Fe-nanoparticles and titania-Fe-nanoparticles were analyzed electron microscopically. In order to broaden the spectrum of the nanoparticles formed here also titania/silica/layer-by-layer-iron nanoparticles, the titania/silica-iron nanoparticles, have been prepared and analyzed.

Scanning electron microscopy (SEM) analysis of the nanoparticles was performed with a Zeiss DSM 962 Digital Scanning Microscope (Zeiss, Aalen; Germany). The samples were mounted onto aluminum stubs (SEM-Stubs G031Z; Plano, Wetzlar; Germany) that were covered with adhesive carbon (carbon adhesive Leit-Tabs G3347). Prior to analysis, the samples were sputtered with a 20-nm-thin layer of gold in argon plasma. The SEM/EDX (energy-dispersive X-ray spectroscopy) analyses were performed as described recently; those samples were not sputtered.[20]

Transmission electron microscopy (TEM) was performed as previously described,[50] using a Philips EM-420:120-kV microscope equipped with a CCD camera.

4.9 *Escherichia coli* culture

E. coli (strain TOP10; Invitrogen) was cultivated in LB-Medium (Luria/Miller #X968.1; Roth, Karlsruhe; Germany). For starting of the experiments, a cells density of 0.2 OD_{600} has been chosen. After an initial incubation period for 60 min the experiments in the Eppendorf test tubes were started by exposing the cultures to ultraviolet (UV) light. After the indicated period of incubation the cultures were removed and the optical density was determined.

Where outlined the bacteria, growing on LB-Medium/LB-Agar (Roth X969.1) and supplemented with 50 µg/mL of nanoparticles, remained either in the dark, or were exposed to the UV-A light (λ_{max}: 365 nm; see below) at a distance of 5 cm from the top of the Petri dish.

4.10 Killing of bacteria by using a magnetic nanoparticle separator

In our home-made apparatus the Eppendorf reaction tube (volume 2 mL) was hooked to a small docking platform (Fig. 6). The cover of the tube was removed and replaced by a socket into which a stainless coil stirrer was fitted. Nanoparticles were filled into the reaction tube, containing the culture medium with the bacteria. The cell suspension was stirred by a motor *via* the coil stirrer. At the end of the incubation the nanoparticles were collected from the incubation assay. The assay system, medium, *E. coli*, and nanoparticles were irradiated, at a distance of 1 cm, with an illuminating UV-A light source (UV-Emitter 365 nm SMD; Star-UV365-10-00-00; λ_{max}: 365 nm; 1600 mW/cm^2, 11 W). This light quality can penetrate the polypropylene tubes with an efficiency of 85 % (information by the Eppendorf company [http://www.eppendorf.com/int/index.php?l=1&action=library&contentid=11&sitemap=4.5.3&listid=9808]).

4.11 Statistical analysis

The results were statistically evaluated using paired Student's *t*-test.[51]

Conclusions

This safe application of titania-Fe-nanoparticles in cleaning of sewage will surely receive positive public attention, also based on the facts that nanoparticles are routinely applied in many different areas, e.g. electronics, biomedicine, pharmaceutics, or cosmetics. Especially, in regenerative medicine the application of iron nanoparticles gain increasing interest and is indispensable; while short-term studies are auspicious, long-term *in vivo* studies are still ongoing. However, it can be expected that the general acceptance of the titania-Fe-nanoparticles for the photocatalytic disinfection in the highly polluted sewage is granted.

In future studies we will develop iron nanoparticles that have the capacity to bind to heavy metal ions in order to broaden the application range of the magnetic nanoparticle separator, described here.

Acknowledgements

W.E.G. M. is a holder of an ERC Advanced Investigator Grant (No. 268476 BIOSILICA). This work was supported by grants from the Deutsche Forschungsgemeinschaft (Schr 277/10-3), the European Commission (Industry-Academia Partnerships and Pathways "CoreShell": No. 286059; "Bio-Scaffolds": No. 604036; "MarBioTec*EU-CN*": No. 268476; and "BlueGenics":

No. 311848), as well as the International Human Frontier Science Program.

Notes and references

[a] *ERC Advanced Investigator Grant Research Group, Institute for Physiological Chemistry, University Medical Center of the Johannes Gutenberg University Mainz, Duesbergweg 6, D-55128 Mainz, GERMANY;E-mail: wmueller@uni-mainz.de (W. E. G. Müller), wang013@uni-mainz.de (X. H. Wang)*
[b] *Institute of Karst Geology, CAGS, No. 50 Qixing Road, 541004-Guilin Guangxi, CHINA*
[c] *Center for Marine Research, Ruđer Bošković Institute, G. Paliaga 5, HR-52210 Rovinj, Croatia*

1 C. T. Yavuz, J. T. Mayo, W. W. Yu, A. Prakash, J. C. Falkner, S. Yean, L. L. Cong, H. J. Shipley, A. Kan, M. Tomson, D. Natelson and V. L. Colvin, *Science*, 2006, **314**, 964.
2 R. K. Zahn, G. Zahn, W. E. G. Müller, I. Müller, R. Beyer, U. Müller-Berger, B. Kurelec, M. Rijavec and S. Britvic, *The Science of the Total Environment*, 1977, **8**, 109.
3 R. K. Zahn, G. Zahn, W. E. G. Müller, M. L. Michaelis, B. Kurelec, M. Rijavec, R. Batel and N. Bihari, *Total Environm.*, 1983, **26**, 137.
4 M. Fafanđel, N. Bihari, V. Krajcar, W. E. G. Müller, R. K. Zahn and R. Batel, *The Science of the Total Environment* 2001, **277**, 149.
5 D. Guin, B. Baruwati and S. V. Manorama, *Org. Lett.*, 2007, **9**, 1419.
6 J. Wang, S. Zheng, Y. Shao, J. Liu, Z. Xu and D. Zhu, *J. Colloid Interface Sci.*, 2010, **349**, 293.
7 C. Chen, P. Gunawan and R. Xu, *J. Mater. Chem*., 2011, **21**, 1218.
8 K. Mandel and F. Hutter, *Nano Today*, 2012, **7**, 485.
9 A. López-Cruz, C. Barrera, V. L. Calero-Ddelc and C. Rinaldi, *J. Mater. Chem.*, 2009, **19**, 6870.
10 S. W. Watson, T. J. Novitsky, H. L. Quinby and F. W. Valois, *Appl. Environ. Microbiol.*, 1977, **33**, 940.
11 M. Breitbart, *Ann. Rev. Mar. Sci.*, 2012, **4**, 425.
12 A. M. Essa, L. E. Macaskie and N. L. Brown, *Biochemical Society Transactions*, 2002, **30**, 672.
13 R. Osinga, H. Belarbi el, E. M. Grima, J. Tramper and R. H. Wijffels, *J. Biotechnol.*, 2003, **100**, 141.
14 W. E. G. Müller, R. Steffen, B. Kurelec, N. Smodlaka, S. Puskaric, B. Jagic, G. Müller-Niklas and N. V. Queric, *Toxicol. & Pharmacol.*, 1998, **6**, 229.
15 J. E. Alouf, *The comprehensive sourcebook of bacterial protein toxins*, Academic Press, London, 2006.
16 I. Arana, P. Santorum, A. Muela and I. Barcina, *Lett. Appl. Microbiol.*, 2000, **31**, 157.
17 J. M. Cobcroft and S. C. Battaglene, *J. Fish Dis.*, 2013, **36**, 57.
18 P. Curnow, P. H. Bessette, D. Kisailus, M. M. Murr, P. S. Daugherty, D. E. Morse, *J. Am. Chem. Soc.*, 2005, **127**, 15749.
19 X. H. Wang, U. Schloßmacher, H. C. Schröder and W. E. G. Müller, *Soft Matter*, 2013, **9**, 654.
20 W. E. G. Müller, H. C. Schröder, U. Schloßmacher, V. A. Grebenjuk, H. Ushijima and X. H. Wang, *Biomaterials*, 2013, **34**, 8671.
21 M. J. Uriz, X. Turon and M. A. Becerro, *Cell Tissue Res.*, 2000, **301**, 299.
22 S. Standeker, Z. Novak and Z. Knez, *J. Colloid Interface Sci.*, 2007, **310**, 362.
23 N. Sakai, Y. Ebina, K. Takada and T. Sasaki, *J. Am. Chem. Soc.*, 2004, **126**, 5851.
24 J. C. Ireland, P. Klostermann, E. W. Rice and R. M. Clark, *Appl. Environ. Microbiol.*, 1993, **59**, 1668.
25 G. Gogniat, M. Thyssen, M. Denis, C. Pulgarin and S. Dukan, *FEMS Microbiol. Lett.*, 2006, **258**, 18.
26 J. Marugan, R. van Grieken, C. Sordo and C. Cruz, *Applied Catalysis B: Environmental*, 2008, **82**, 27.
27 E. F. Duffy, F. Al Touati, S. C. Kehoe, O. A. McLoughlin, L. Gill, W. Gernjak, I. Oller, M. I. Maldonado, S. Malato, J. Cassidy, R. H. Reed and K. G. McGuigan, *Sol. Energy*, 2004, **77**, 649.
28 S. Bonetta, S. Bonetta, F. Motta, A. Strini and E. Carraro, *AMB Express*, 2013, **3**, 59.
29 A. A. Sawyer, D. M. Weeks, S. S. Kelpke, M. S. McCracken and S. L. Bellis, *Biomaterials*, 2005, **26**, 7046.
30 S. Sun and H. Zeng, *J. Am. Chem. Soc.*, 2002, **124**, 8204.
31 J. Park, K. An, Y. Hwang, J. G. Park, H. J. Noh, J. Y. Kim, J. H. Park, N. M. Hwang and T. Hyeon, *Nat. Mater.*, 2004, **3**, 891.
32 T. A. Egerton, S. A. Kosa and P. A. Christensen, *Phys. Chem. Chem. Phys.*, 2006, **8**, 398.
33 A. Fujishima and K. Honda, *Nature*, 1972, **238**, 37.
34 O. Legrini, E. Oliveros and A. M. Braun, *Chem. Rev.*, 1993, **93**, 671.
35 M. M. Halmann, *Photodegradation of Water Pollutants,* CRC Press, Boca Raton, 1996.
36 A. Mills and S. Le Hunte, *J. Photochem. Photobiol. A: Chem.*, 1997, 108, 1.
37 D. F. Ollis and H. El-Akabi, *Photocatalytic Purification and Treatment of Water and Air*, Elsevier Science, Amsterdam, 1993.
38 J. W. Liou and H. H. Chang, *Arch. Immunol. Ther. Exp.*, 2012, **60**, 267.
39 A. R. Mahdavian and M. A.-S. Mirrahimi, *Chem. Engineer. J.*, 2010, **159**, 264.
40 H. Markides, M. Rotherham and A. J. El Haj, *J. Nanomat.*, 2012, **2012**, doi:10.1155/2012/614094.
41 W. E. G. Müller, X. H. Wang, V. A. Grebenjuk, M. Korzhev, M. Wiens, U. Schloßmacher and H. C. Schröder, *PLoS ONE*, 2012, **7(4)**, e34617, doi:10.1371/journal.pone.0034617.
42 A. Krasko, B. Lorenz, R. Batel, H. C. Schröder, I. M. Müller and W. E. G. Müller, *Europ. J. Biochem.*, 2000, **267**, 4878.
43 F. Natalio, T. Link, W. E. G. Müller, H. C. Schröder, F. Z. Cui, X. H. Wang and M. Wiens, *Acta Biomaterialia*, 2010, **6**, 3720.
44 U. Schloßmacher, M. Wiens, H. C. Schröder, X. H. Wang, K. P. Jochum and W. E. G. Müller, *FEBS J.*, 2011, **278**, 1145.
45 X. Tong, T. Tang, Z. Feng and B. Huang, *J. Appl. Polym. Sci.*, 2002, **86**, 3532.
46 K. Shimizu, J. Cha, G. D. Stucky and D. E. Morse, *Proc. Natl. Acad. Sci. USA*, 1998, **95**, 6234.
47 R. De Palma, S. Peeters, M. J. Van Bael, H. Van den Rul, K. Bonroy, W. Laureyn, J. Mullens, G. Borghs and G. Maes, *Chem. Materials*, 2007, **19**, 1821.
48 M. Wiens, T. Link, T. A. Elkhooly, S. Isbert and W. E. G. Müller, *ChemComm*, 2012, **48**, 11331.
49 W. E. G. Müller, M. Rothenberger, A. Boreiko, W. Tremel, A. Reiber and H. C. Schröder, *Cell Tissue Res.*, 2005, **321**, 285.
50 W. E. G. Müller, A. Boreiko, U. Schloßmacher, X. H. Wang, M. N. Tahir, W. Tremel, D. Brandt, J. A. Kaandorp and H. C. Schröder, *Biomaterials*, 2007, **28**, 4501.
51 L. Sachs, *Angewandte Statistik*, Springer, Berlin, 1984, p. 242.